We are IntechOpen, the world's leading publisher of Open Access books Built by scientists, for scientists

6,900
Open access books available

186,000
International authors and editors

200M
Downloads

Our authors are among the

154
Countries delivered to

TOP 1%
most cited scientists

12.2%
Contributors from top 500 universities

CLARIVATE ANALYTICS
BOOK CITATION INDEX
INDEXED

WEB OF SCIENCE™

Selection of our books indexed in the Book Citation Index
in Web of Science™ Core Collection (BKCI)

Interested in publishing with us?
Contact book.department@intechopen.com

Numbers displayed above are based on latest data collected.
For more information visit www.intechopen.com

Major Chemical Elements in Soot and Particulate Matter Exhaust Emissions Generated from In-Use Diesel Engine Passenger Vehicles

Richard Viskup, Christoph Wolf and Werner Baumgartner

Abstract

In this research we apply a sensitive laser optical technique for the measurement of main chemical elements present in the exhaust emissions generated from different in-use Diesel engine passenger vehicles. We use the laser-induced breakdown spectroscopy (LIBS) technique for diagnostics of miscellaneous Diesel particulate matter (DPM) formed from combustion Diesel engine exhaust emissions. Here we analysed particulate matter (PM) extracted from exhaust manifold part, from 67 different passenger vehicles of major brands from European car producers, that are used in daily life environment. The aim of this study is to develop LIBS technique for measurement of PM and to compare the emission matrix composition and major chemical elements within the Diesel particulate matter from exhaust manifold part. The presence of these elements in PM is linked with various processes inside the Diesel combustion engine.

Keywords: laser-induced breakdown spectroscopy, LIBS, particulate matter, soot, emissions, emissions standards, diesel, diesel engine, diesel vehicles

1. Introduction

Problems with Diesel emissions and control failures [1–3] are well known to anyone in the world. Breathing of clean air is very important for a healthy human body—mainly for the brain and nervous system. Therefore, it should be in our first priority to find a new technique to successfully solve these issues. The current existing emission standards in Europe, like European emission standards Euro [4, 5], or in the US, like Tier [6] or LEV [7], for Diesel engine passenger vehicles are the norms for hydrocarbons, carbon monoxide, nitrogen oxides, and particulate matter (PM) from Diesel exhaust emissions. Currently, there are no specific emission standards for additional compounds or chemical elements contained in the exhaust vapour [8], particulate matter [9, 10], or soot, formed by the Diesel combustion engine [11]. But in fact, the composition of chemical elements and extra carbon corresponds to a very important fraction of the total PM or black soot emission contents from Diesel engine-driven vehicles. **Figure 1** shows the black cloud of Diesel exhaust emissions emitted from the tail pipe of on-road Diesel engine passenger vehicle.

One of the early pioneering groups in measurement of particulate trace emissions from vehicles was the group of Schauer et al. [9], where they used comprehensive

Figure 1.
Black cloud of particulate matter and soot exhaust emissions from the tail pipe of on-road diesel engine passenger vehicle.

dilution source sampler, organic chemical analysis, and X-ray fluorescence for fine particle mass and chemical composition measurements. Other groups [8, 10–12] used ICP-MS and XRF for characterisation of metals and other components from on-road motor vehicles. They found the following trace elements: Al, Ba, Be, Ca, Cd, Co, Cr, Cu, Fe, K, Mg, Mn, Mo, Na, Ni, Pb, Pt, S, Sr, Ti, V, and Zn in the particles.

In this research we apply the laser-induced breakdown spectroscopy (LIBS) technique [13–15] for diagnostics of DPM, formed from combustion Diesel engine exhaust emissions, mainly concerning the comparison of major chemical components present in various DPM matrices.

Laser-induced breakdown spectroscopy is an emerging measurement technique [16] for rapid qualitative [17] and sensitive quantitative compositional analysis [18, 19] of various forms of materials like solids [20], liquids [21], gases [22], powders [23], or nanoparticles [24].

2. Materials and methods

2.1 Experimental procedure

An experimental setup, used to obtain LIBS spectra from various materials, generally consists of a high-intensity pulsed laser system, with nanosecond laser pulse duration, an experimental chamber, a collection optics, and a high-precision optical spectrometer. Plasma is generated by focusing the high-intensity laser pulses into the material; usually a Nd:YAG laser is applied at its fundamental laser wavelength of 1064 nm or its second harmonic 532 nm with different repetition rates from 1 Hz to a few kHz [25–27]. A schematic of the experimental LIBS setup is shown in **Figure 2**.

2.2 LIBS setup

For laser-induced breakdown, a Nd:YAG solid-state laser from Quantel was used. It was operated at the fundamental laser wavelength 1064 nm with 8.5 ns pulse duration and a laser energy of 300 mJ per pulse. The laser radiation was focused into the plane solid target surface, using a 10 cm focusing lens, to create the plasma. Optical emission from the plasma was collected perpendicularly via optical telescope, into the high-resolution Echelle spectrograph (model Aryelle Butterfly from LTB Berlin), equipped with an ICCD detector. Optical emission from plasma has been collected from UV as well as from VIS parts; thus the total spectral window from 190 to 800 nm wavelength has been recorded. The spectral resolution capability is from 3 to 7 pm for the UV range and from 4 to 8 pm for the VIS range, thus providing spectral information of a
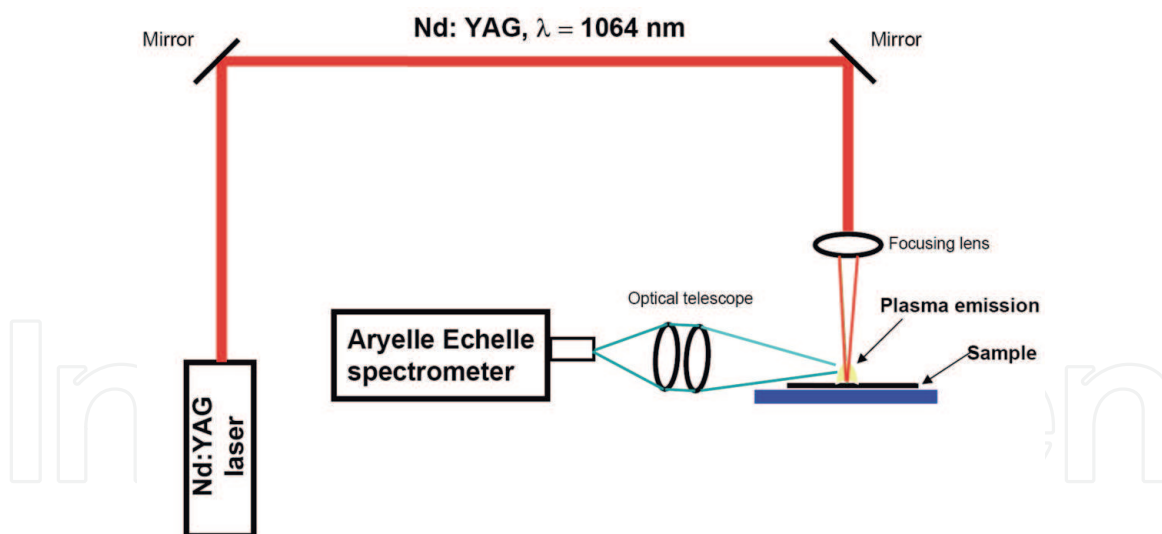
Figure 2.
Layout of the laser-induced breakdown spectroscopy experimental setup [28].

broad range with very high resolution and variability. The delay time for LIBS spectral signal was set to 1 μs and the time window for spectral acquisition to 2 μs. In early delay time, less than 1 μs, the black body radiation is dominating in the laser-produced plasma, while in later delay time, 3 μs, the atomic, ionic, and molecular emissions are more pronounced. The laser-induced plasma has been created in open air atmosphere under the normal atmospheric pressure and at room temperature.

2.3 Diesel particulate matter (DPM) collection and sample preparation

Sixty-seven different PM samples, extracted from exhaust manifold part from in-use Diesel engine passenger vehicles of major brand car producers in Europe, have been analysed by LIBS. Passenger vehicles selected for the DPM sample collection were from our daily life environment, as anyone is using to drive to work, etc. No special driving test cycles, neither test vehicles nor engine test bench systems, were used during these LIBS measurements. Diesel particulate matter has been collected and extracted from the exhaust manifold part tail pipe at the end of the exhaust manifold. Selections of the vehicles were performed randomly, and no company was given preference. The results presented here are from a selection of eight different DPM matrices with respect to the LIBS signal variation. The reason is to compare the elemental composition of these different DPM matrices by LIBS technique. A special emphasis is given to observe the individual spectral lines that are mostly dominating in the UV and VIS optical emission from the DPM, thus influencing the overall LIBS spectrum. The collected DPM from Diesel engine vehicles' exhaust has been mechanically pressed into pellets with a flat disc shape. Each displayed spectrum has been averaged over 12 laser shots.

3. Results and discussion

3.1 Identification of the main chemical elements in different DPM matrices

For an elemental understanding of the laser-induced breakdown spectroscopy signal from DPM in the first stage, we selected from 67 different samples only 3 LIBS optical emission spectra. Signals from these measurements are shown in **Figure 3**. Obtained LIBS spectra have characteristic features with strong atomic and ionic lines and also molecular bands in the signal.

Pressed solid samples of DPM were irradiated by high-power laser pulses to create a plasma above the surface. The optical emission from laser-induced plasma has been measured, and the raw spectral signal from 200 nm to 800 nm is plotted in the **Figure 3**. The major signal that is present in the LIBS spectrum is characterised by strong optical emission lines from the elements carbon, calcium, iron, chromium, sodium, zinc, aluminium, magnesium, oxygen, and hydrogen. These chemical elements show up in the spectrum as high-intensity lines. The relative intensity and broadening of the spectral lines are correlated with the chemical concentration of the elements. That means with higher intensity of atomic and ionic lines, we can expect a higher concentration of the studied chemical element.

In the next section, we will focus our study on the chemical elements and spectral lines that are most abundant in the LIBS spectra under investigation. Optical emission spectra of C, Ca, Fe, Cr, Na, Zn, Al, Mg, O, and H measured from 67 different Diesel particulate matter samples are shown in **Figure 4**. Spectra shown here are selections of the most dominant lines in the signal. PM were collected from 67 different in-use Diesel engine passenger vehicles.
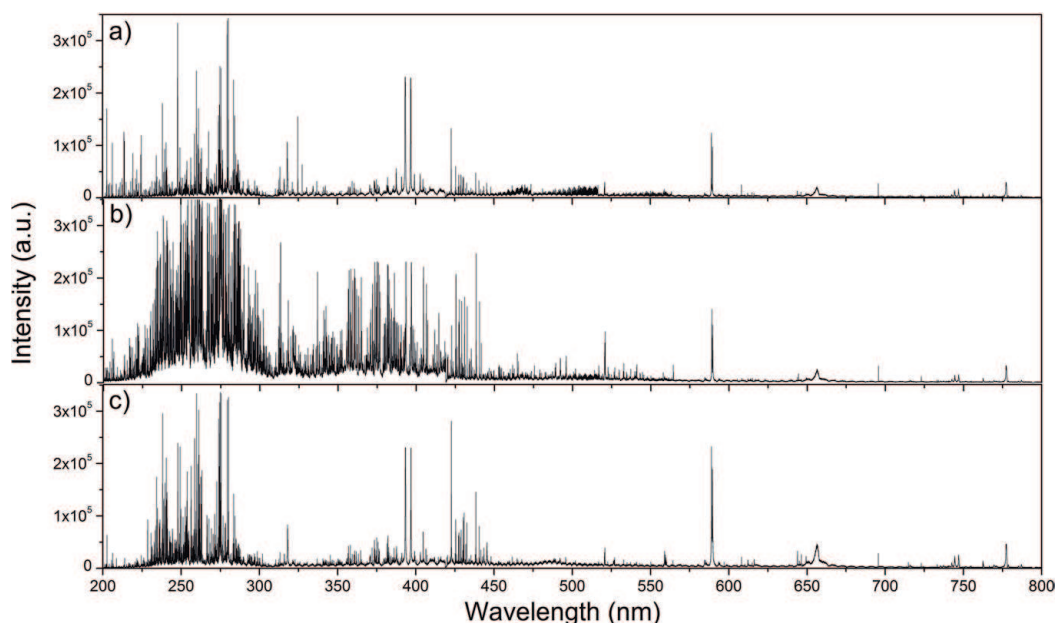

Figure 3.
LIBS spectra from three selected Diesel Particulate Matter samples, with high content of a) Ca, Mg, Zn; b) Ca, Cr, Fe, H, Mg, Na and c) Al, C, Ca, Cr, Mg, O.

3.1.1 Carbon spectral line

In **Figure 4a** a comparison of the atomic carbon spectral line C I at 247.85 nm optical emission from different particulate matter matrices measured by LIBS is shown. One can easily observe that the peak intensity, peak shape, and peak width vary for each obtained spectrum. Samples with high content of iron particles possess an additional iron peak Fe II at 248.015 nm interfering with the carbon signal line C I at 247.85 nm. Here, it is obvious that the line emission from carbon is not the only dominant spectral line in the LIBS signal.

3.1.2 Calcium spectral line

An important major chemical component of the DPM is calcium. A comparison of LIBS signals from calcium (atomic spectral line Ca I at 422.67 nm) is shown in **Figure 4b**. Calcium emission shows to be always present in DPM samples, and

due to its strong optical emission, it can be assumed as one of the main components of the DPM matrix.

3.1.3 Iron spectral line

In **Figure 4c** comparisons of the ionic optical emission from iron spectral line Fe II at 238.20 nm are shown. Additional four iron spectral lines are also visible in the graph: Fe II at 237.92 nm, Fe II at 238.07 nm, Fe II at 238.32 nm, and Fe II at 238.43 nm. From the shown optical iron spectra, one can clearly see that the iron content is quite high in many PM samples. Iron is one of the components that is often present in the Diesel particulate matter and plays an important role in PM composition. High concentrations of iron are responsible for the transition of the DPM matrix.

3.1.4 Chromium spectral line

In **Figure 4d** comparisons of the optical emission from atomic chromium triplet lines Cr I at 520.44 nm, Cr I at 520.60 nm, and Cr I at 520.84 nm obtained from different DPM samples are shown. The presence of chromium is significant in most of the samples and therefore plays an important role in PM composition.

3.1.5 Sodium spectral line

Comparisons of the optical emissions from sodium atomic doublet spectral line (Na I at 588.99 nm and Na I at 589.59 nm) are shown in **Figure 4e**. Sodium is one of the elements that are perpetually present in the DPM matrix. The sodium atomic line intensity is relatively high and is dominating in the optical infrared spectrum. Thus it also plays an important role in the DPM content.

3.1.6 Zinc spectral line

Comparisons of the zinc ionic spectral line (Zn II at 202.54 nm) are shown in **Figure 4f**. Optical emission from zinc is usually present in all DPM samples. However, the intensity of Zn-induced emission is quite high in some individual samples, which is related to a high zinc content. It is therefore expected that the element Zn also influences the DPM matrix.

3.1.7 Aluminium spectral line

In **Figure 4g** optical emissions from atomic aluminium, Al I at 309.27 nm line, are shown. Aluminium-induced optical emission is strongly present in a few DPM samples, and this high peak in the LIBS signal is indicating higher concentrations of Al in these matrices.

3.1.8 Magnesium spectral line

In **Figure 4h**, emissions from the doublet of ionic magnesium spectra lines (Mg II at 279.55 nm and Mg II at 280.27 nm) are shown. From these spectra it is possible to observe that magnesium lines are present in most of the particulate matter.

3.1.9 Oxygen spectral line

Strong signal from the atomic oxygen line (O I at 777.19 nm) in **Figure 4i** is visible from all DPM samples. This signal is partially due to laser-induced breakdown in air
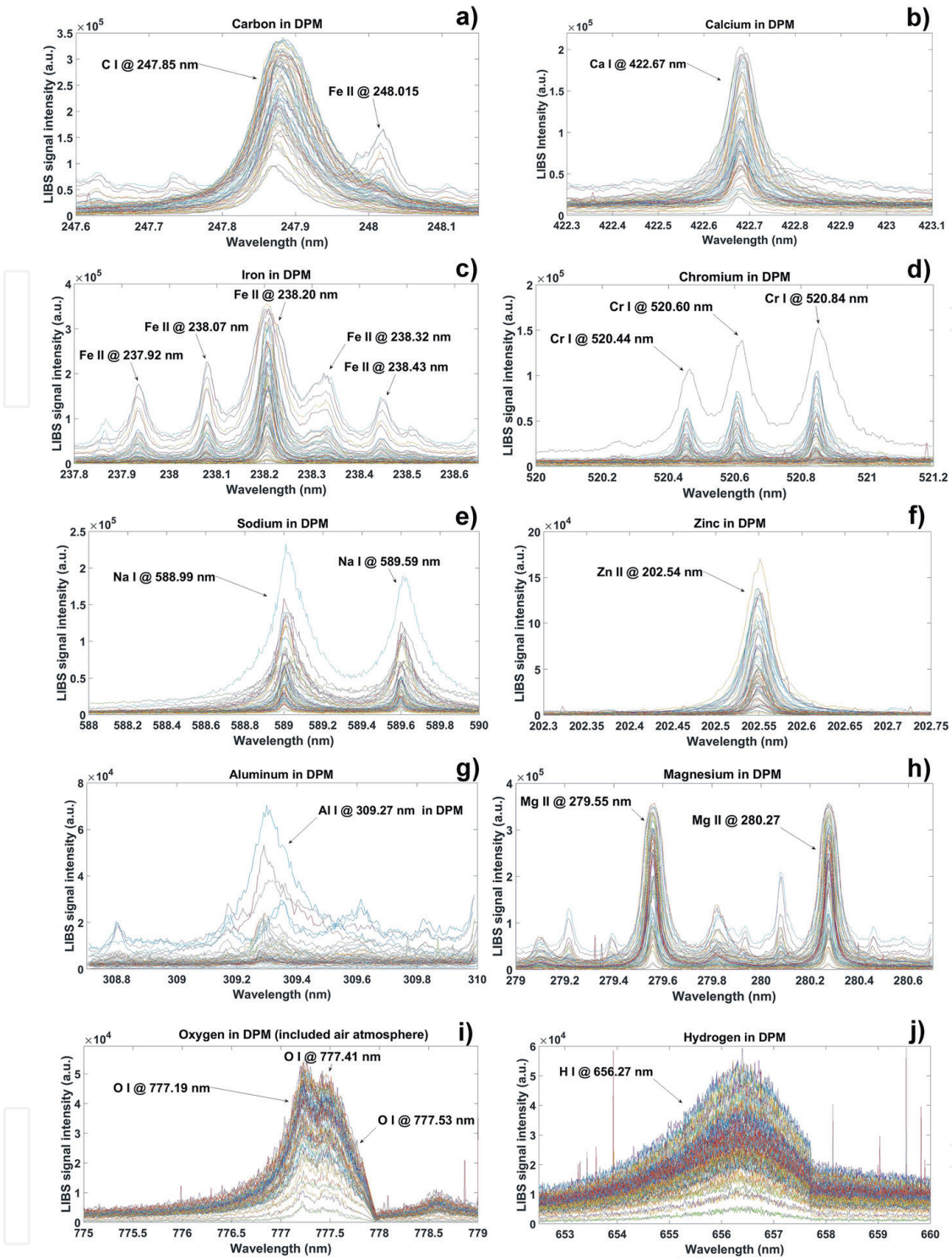
Figure 4.
Optical emission spectrum of (a) carbon, (b) calcium, (c) iron, (d) chromium, (e) sodium, (f) zinc, (g) aluminium, (h) magnesium, (i) oxygen, and (j) hydrogen, measured by LIBS from 67 different diesel particulate matter samples.

atmosphere; nevertheless the other contribution in the signal is from residual oxygen present in the particulate matter. In some cases, this signal is very intense, indicating rather high concentrations of oxygen or different oxides in the sample itself.

3.1.10 Hydrogen spectral line

A very important indicator is the hydrogen H I at 656.27nm line profile in the laser-induced plasma emission. From Balmer series H alpha line and from Stark

broadening, the concentration of the plasma electron density can be calculated. Further H alpha line intensity and width can be used for electron temperature estimation. In **Figure 4j** one can observe that H(α) has enormous intensity and broadening variations across different DPM matrices.

The chemical composition of individual DPM matrices varies considerably. This is due to the different origins of each particulate matter, which is given by the unique originality of the exhaust emission. In fact, the source of different elemental compositions of this matrix is the combination of the Diesel fuel, fuel additives, composition of the intake air, quality of the combustion process, type and performance of the Diesel engine, lubrication oil, erosion on the piston rings, or cylinder liner. Other parts that influence the matrix composition are applied pretreatment and after-treatment devices, like Diesel particle filters (DPF) or catalysts like selective catalytic reduction devices. All of them are involved in the final chemical composition of DPM.

3.2 Calculation of the LIBS signal

To process LIBS spectral signals, we integrated the spectral peak area for each atomic or molecular line shown in **Figure 4**. With numerical integration, we obtained relative qualitative information about concentration variations of major chemical elements inside the different Diesel particulate matter matrices. Results from these calculations are shown in **Figure 5**. In the bar graph, individual columns represent the calculated integral values of accumulated signal responses obtained for each particular wavelength, after the signal background correction and the fitting of spectral signal curve. Integral calculated values are for 67 DPM samples and for 10 major chemical elements. These are carbon, calcium, iron, chromium, sodium, zinc, aluminium, magnesium, oxygen, and hydrogen.

The carbon signal (**Figure 5a**) in individual Diesel particulate matter samples varies substantially, and these variations influence the entire matrix composition. In some samples, the signal from carbon dominates, which indicates carbon as a major element in these matrices, while in other samples, the influence of carbon is much lower. From an integral calculation, carbon has been detected in all 67 DPM samples. Very high carbon content was measured in samples # 45, 44, 39, and 42, while very low content was detected in samples # 67, 3, and 8.

The calcium (**Figure 5b**) concentration in PM can be quite high. This is visible in **Figure 5** where the integral values are shown. High content of calcium is present in samples # 66, 67, and 25. The minimum content of calcium was found in samples # 55, 11, and 39. Calcium has been detected in 66 of the 67 samples.

The most significant contribution to the entire PM composition comes from iron (**Figure 5c**). Iron has been detected in 66 out of 67 different DPM samples. From **Figure 5**, maximum content of iron was found in samples # 55, 12, 58, 59, and 34. Minimum content has been measured in samples # 37, 13, 2, 53, 30, 11, and 3.

Chromium (**Figure 5d**) content also plays a major role in DPM matrices. Its presence has been measured in 60 from 67 different DPM samples. Its maximum concentration has been measured in samples # 59, 4, 12, 28, 34, and 50. Minimum concentration of Cr has been measured in samples # 9, 13, 17, 24, 30, 55, and 58.

Sodium (**Figure 5e**) can reach relatively high values in some samples, mainly in # 54, 59, 27, and 12. Minimum concentration of Na was found in # 39, 11, 48, 30, and 15. Overall, sodium has been detected in almost all samples (66/67).

Zinc (**Figure 5f**) is another important major element in various Diesel particulate matter matrices. Its concentration can be quite high, as we can observe in samples # 44, 37, 18, 35, 33, 41, 52, and 5. On the other hand, low concentrations of
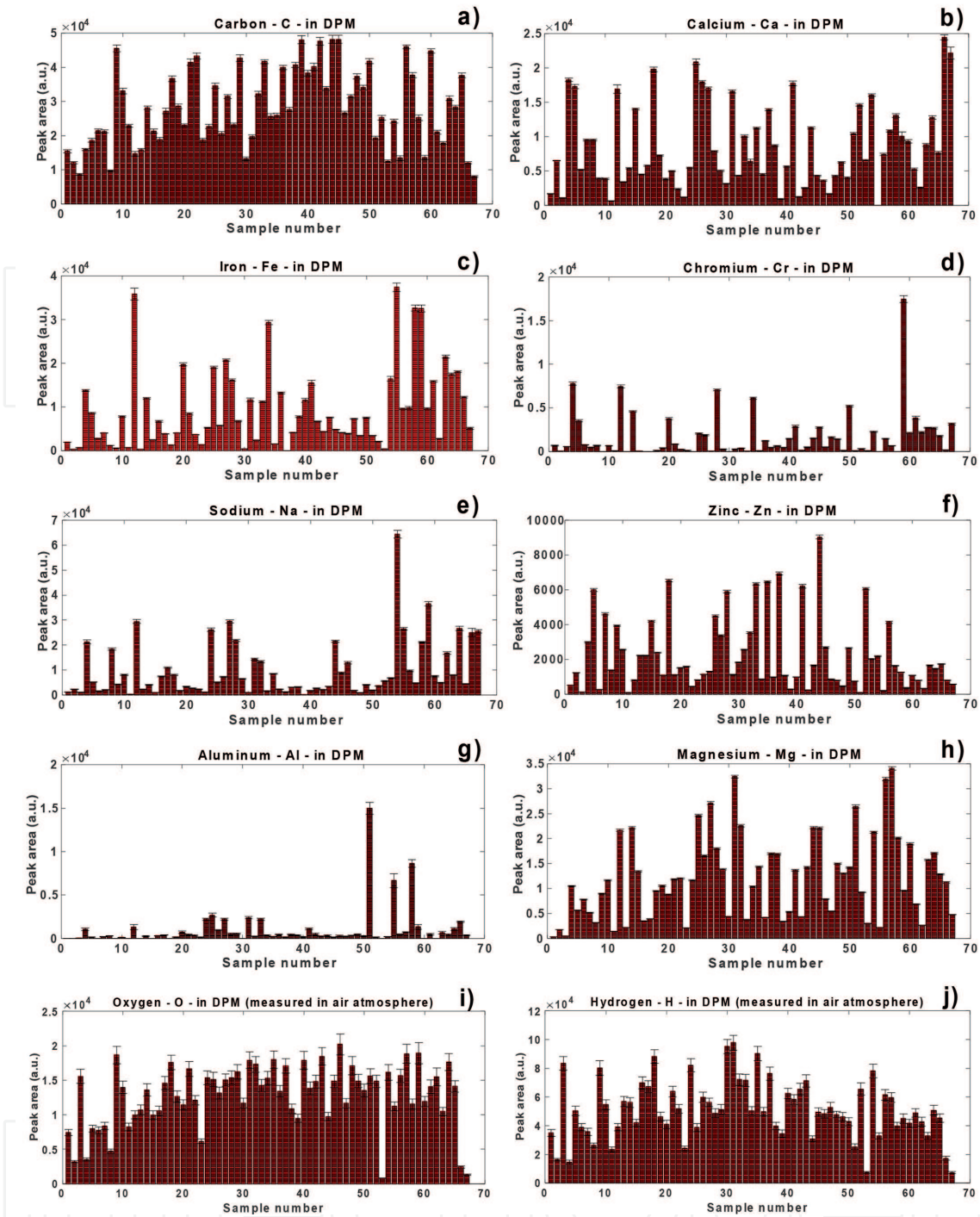
Figure 5.
Qualitative comparison of (a) carbon, (b) calcium, (c) iron, (d) chromium, (e) sodium, (f) zinc, (g) aluminium, (h) magnesium, (i) oxygen, and (j) hydrogen content in DPM from 67 different in-use diesel engine passenger vehicles measured by LIBS.

Zn were measured in 51, 11, 30, 55, 42, and 39. Zinc content has been detected in all 67 different DPM samples.

Three samples of DPM possess higher content of aluminium (**Figure 5g**), particularly samples # 51, 58, and 55. Lower content of Al has been measured in # 1, 2, 3, 6, 9, 11, 13, 15, 18, 30, 53, 60, and 62. Aluminium has been detected in 54 samples.

A major fraction in the DPM composition consists of magnesium (**Figure 5h**). Its high concentrations were measured in samples # 57, 31, 56, 27, 51, and 25. Lower concentrations of Mg were found in # 1, 3, 11, 2, 23, and 55. Magnesium has been ascertained in all 67 DPM samples.

Oxygen (**Figure 5i**) contribution in DPM is meaningful, and its content forms a major part in matrices. Oxygen has been detected in all samples, with high

concen-trations in # 46, 9, 59, and 57 and with lower concentrations in samples # 53, 67, 66, 2, and 4.

Hydrogen (**Figure 5j**) content is likewise very substantial in DPM. It is a major chemical element of DPM and it has been detected in all samples. High concentrations were measured in samples # 31, 30, 35, 18, 3, 24, 9, 54, and 37; while low content in samples # 53, 67, 4, and 2.

3.3 Quantitative diesel particulate matter analysis

Every knowledge about the qualitative and quantitative atomic composition of the studied material is contained in the LIBS spectrum. This originates from excited atoms, ions, and molecules, in the laser-induced plasma. Different methods exist to extract quantitative information from LIBS spectra. One technique determines the concentration of chemical elements by calculation of the line spectral emission from transition probabilities and from absolute measurements of the line intensities. A different strategy is to calculate, from the obtained signal, the integral of the emission line relative to the integral of a spectral line from the abundant element. Quite often approaches to get quantitative results are the spectral intensities in relation to known calibration standards or certified reference materials. By assuming the optical emission line intensity to be proportional to the concentration of the emission inducing species, the ratio of the concentrations of two species A and B can be expressed as a function ratio of the line intensity of species A to the line intensity of species B. Considering that the concentration ratio is directly proportional to the ratio of corresponding line intensities, it is possible to establish a calibration curve. This curve is basically a plot of relative concentrations of an element obtained by LIBS measurements versus the known relative concentrations of this element in the samples. Calibration curves can then be used for the quantitative determination of unknown concentrations in the examined material.

Special concern has been given to the quantification of the LIBS spectral signal and to the calibration curves from selected main matrix elements of DPM. The calibration function for carbon, iron, magnesium, aluminium, chromium, zinc, sodium, and calcium was constructed, to understand the complex composition of DPM.

3.3.1 Preparation of the calibration samples

To obtain quantitative information from the LIBS signal, calibration samples with various concentrations of expected chemical elements were prepared. We selected the elements carbon, iron, magnesium, aluminium, chromium, zinc, sodium, and calcium that form the major part of DPM matrix. Based on our previous qualitative LIBS measurements of different DPM matrices, we produced similar matrices, in our laboratory. These have been compounded by preparing different mixtures of selected elements in various concentrations and pressing them into pellets, exactly like the original DPM samples. All calibration samples have been prepared from certified nano-powders bought either from Carl Roth GmbH or from Sigma-Aldrich Inc. Company.

3.3.2 Measurement of calibration samples by LIBS

The calibration samples were measured under the same experimental conditions as the DPM samples. Consistent experimental parameters as optical setup, laser energy, spectrometer detector settings, particularly spectral window, and delay
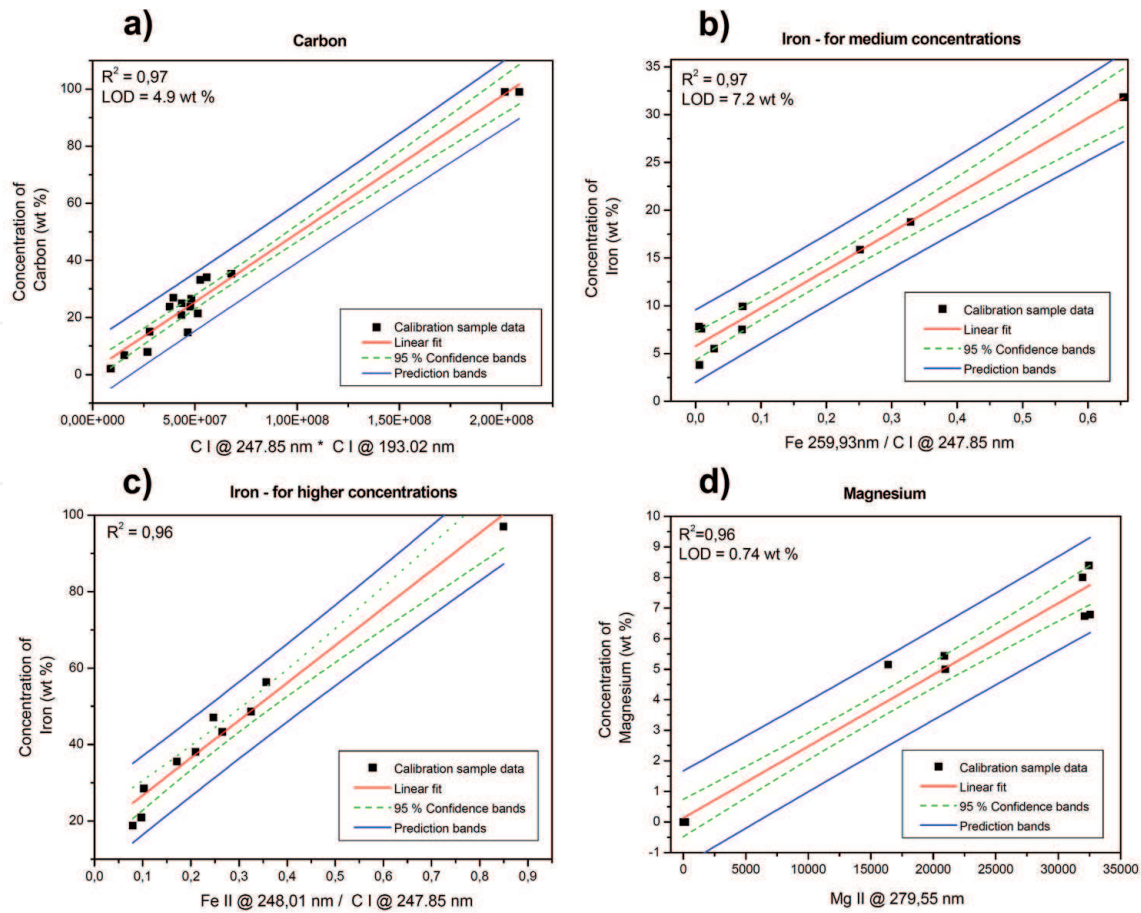
Figure 6.
Calibration curves including regression parameter R², limit of detection (LOD), 95% confidence limits, and prediction bands for (a) carbon, (b) iron (medium concentrations), (c) iron (high concentrations), and (d) magnesium calibration samples.

time remained unchanged. Experimental LIBS measurements were performed in air atmosphere at normal atmospheric pressure. Obtained calibration curves (together with calculated regression parameter R^2, limit of detection (LOD), 95% confidence limits, and prediction bands) for (a) carbon, (b) iron (medium concentrations), (c) iron (high concentrations), (d) magnesium, (e) aluminium, (f) chromium, (g) zinc, (h) sodium, and (i) calcium, in the laboratory-prepared PM calibration samples, are shown in **Figure 6(a–d)** and **Figure 7(e–i)**.

In these figures, the calculated ratios are denoted in the graphs as black squares, linear fit by solid line (red), 95% confidence limits by dashed lines (green), and prediction bands by solid lines (blue). It is important to mention that the LOD for elemental carbon is relatively high. This is due to the fact that we assume DPM as a carbon-dominated matrix. Therefore, this calibration protocol is not intended to be applied to low carbon concentrations. The obtained calibration curve will yield the possibility to predict the level of carbon concentrations in various Diesel particulate matrices.

Selected spectral lines used for calculation of LIBS signal, obtained regression parameters R^2 together with LOD, and calibration functions for different chemical elements are summarised in **Table 1**.

3.4 Quantitative composition of eight different DPM matrices

By means of calibration functions and the DPM-LIBS signal, it is possible to obtain the quantitative information and distribution of major chemical elements in Diesel particulate matter from different in-use Diesel engine passenger vehicles.
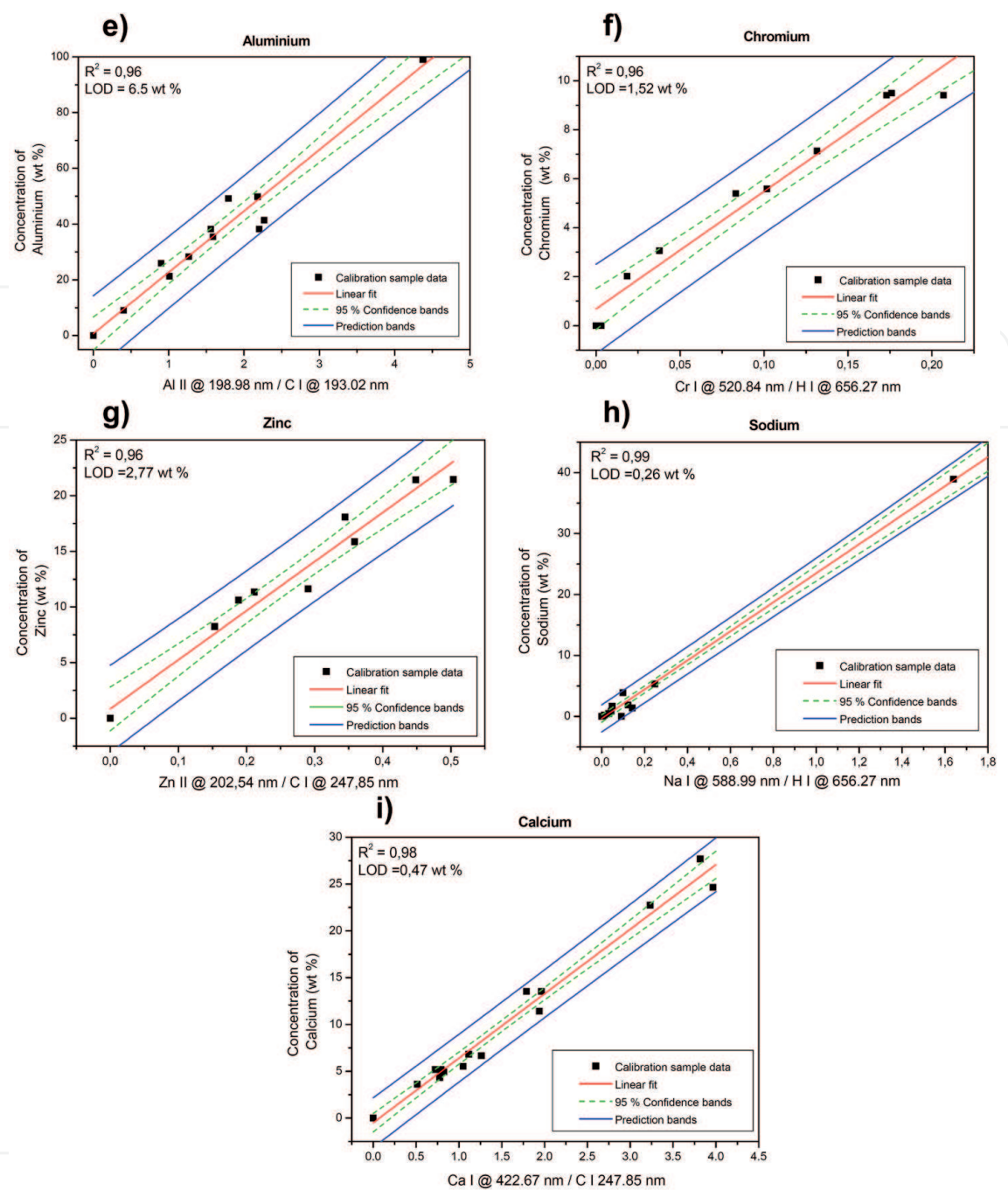
Figure 7.
Calibration curves including regression parameter R^2, limit of detection (LOD), 95% confidence limits, and prediction bands for (e) aluminium, (f) chromium, (g) zinc, (h) sodium, and (i) calcium calibration samples.

Analyte	Regression parameter R^2	LOD (wt %)	Spectral lines used for calculation
C	0.97	4.9	C I @ 247.85nm, C I @ 193.02nm
Fe medium wt%	0.97	7.2	Fe II @ 259.93nm, C I @ 247.85nm
Fe high wt%	0.96	-	Fe II @ 248.01 nm, C I @ 247.85 nm
Mg	0.96	0.74	Mg II @ 279.55nm
Al	0.96	6.5	Al II @ 198.98nm, C I @ 193.02nm
Cr	0.96	1.52	Cr I @ 520.84nm, H I @ 656.27nm
Zn	0.96	2.77	Zn II @ 202.54nm, C I @ 247.85nm
Na	0.99	0.26	Na I @ 588.99nm, H I @ 656.27nm
Ca	0.98	0.47	Ca I @ 422.67nm, C I @ 247.85nm

Table 1.
Selected spectral lines of chemical elements, regression parameter R^2, and limit of detection (LOD) from calculated calibration functions.

In this case, we only present the results from eight of the most diverse DPM matrices with respect to the LIBS spectrum, to demonstrate the quantitative comparison of elemental compositions of DPM using laser-induced break-down spectroscopy technique. From qualitative LIBS measurements, these eight samples were characterised to have high content of certain chemical elements: sample #1 with high content of Cr, sample #2 with high content of Ca, sample #3 with high content of Zn, sample #4 with high content of C, sample #5 with high content of Na, sample #6 with high content of Fe, sample #7 with high content of Mg, and sample #8 with
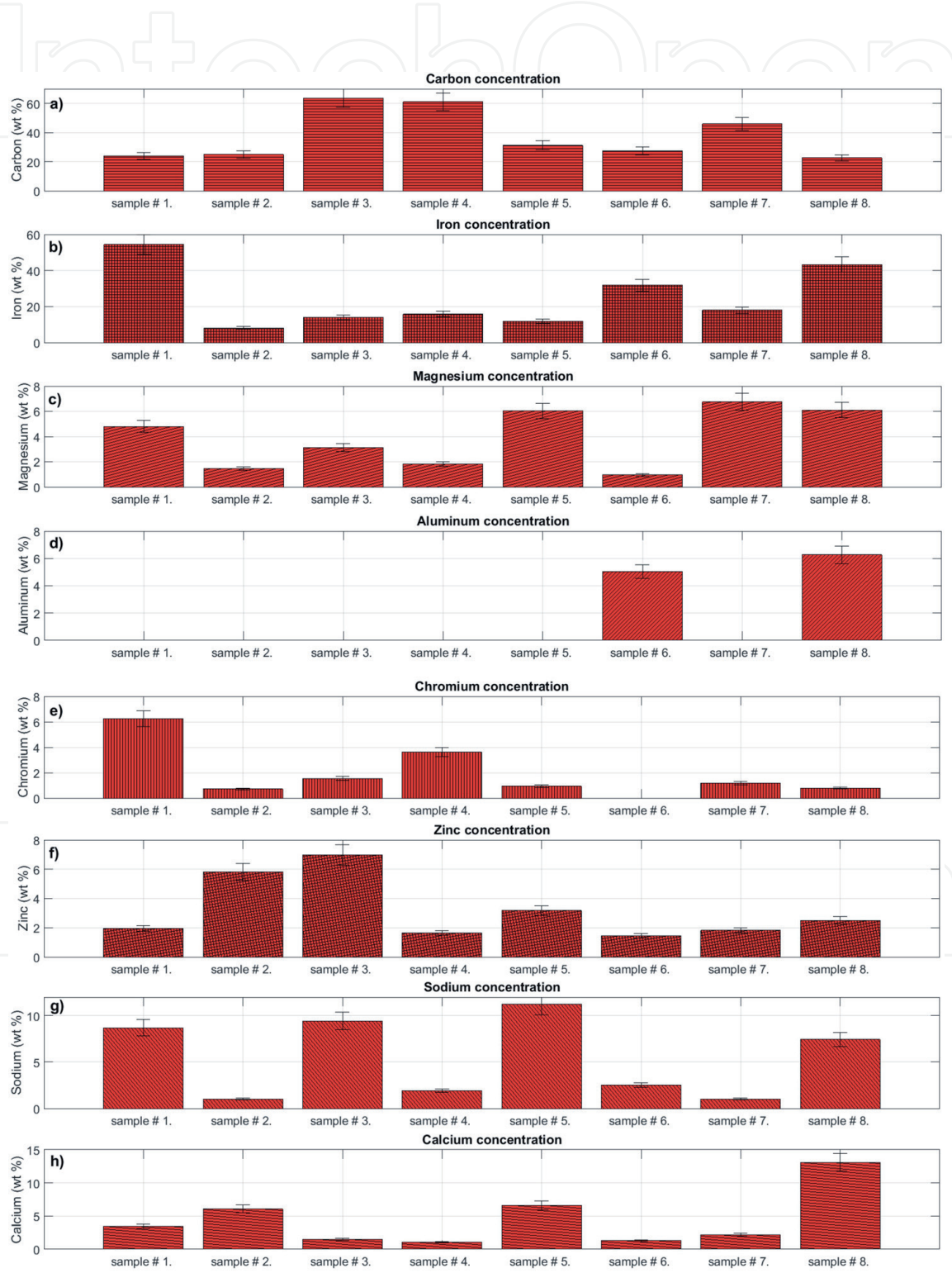

Figure 8.
Quantitative determination of major chemical elements in particulate matter collected from in-use Diesel engine passenger vehicles. The bar graph shows the average concentrations of major element in wt % of (a) carbon, (b) Iron (c) magnesium, (d) aluminium, (e) chromium, (f) zinc, (g) sodium and (h) calcium in eight different DPM samples.

high content of Al. These quantitative determinations of major chemical elements in DPM samples from eight in-use Diesel engine passenger vehicles are shown in **Figure 8(a–h)**.

In the bar graph (**Figure 8(a–h)**), each individual bar represents the average value of calculated concentrations. These average values were obtained from three different position measurements by LIBS at the same DPM sample. The quantitative concentration of each element has been determined from spectral line ratios by means of calibration curves, obtained for each element. The quantitative determination of major chemical elements is shown in weight percent (wt%) in each sample. From the bar graphs, it is possible to obtain quantitative information about the major chemical element concentrations and variations of the DPM chemical composition. The following information can be read by either horizontal or vertical reading of **Figure 8(a–h)**:

From horizontal reading of the bar graph (**Figure 8(a–h)**), it is possible to observe that the carbon concentration (a) is not constant for all DPM samples; instead it is changing rather extremely in between individual samples, ranging from maximum concentration (approximately 64 wt%) to minimum concentration (22 wt%), in different DPM matrices. Iron (b) concentration also varies significantly, from as high as 55 wt% to as low as 8 wt%. Magnesium (c) content is maximum 7 wt% and minimum 1 wt%. Some DPM shows higher value of aluminium (d) with more than 6 wt%, meanwhile for some samples, the Al concentration can be zero. Almost all (except for one) samples contain chromium (e) with minimum concentration below 1 wt%, while maximum can be more than 6 wt%. The zinc (f) content is playing a dominant role within the DPM matrices with concentrations from 1 wt% up to 7 wt%. The sodium (g) concentration also influences the DPM matrices with its concentrations reaching 12 wt%. Calcium (h) concentrations are substantial and can be more than 13 wt%.

From vertical reading of **Figure 8**, one can gain information about average concentrations (due to LIBS measurements at different sample position and averaging) of chemical elements in each DPM sample.

Sample #1: contains in average iron ~54 wt%, carbon ~23 wt%, sodium ~8 wt%, chromium ~6 wt%, magnesium ~5 wt%, calcium ~3 wt%, and zinc ~2 wt%.

Sample #2: contains carbon ~25 wt%, iron ~8 wt%, calcium ~6 wt%, zinc ~6 wt%, magnesium ~1 wt%, sodium ~1 wt%, chromium ~1 wt%, and other elements.

Sample #3: contains carbon ~63 wt%, iron ~14 wt%, sodium ~9 wt%, zinc ~7 wt%, magnesium ~3 wt%, chromium ~1 wt%, calcium ~1 wt%, and other elements.

Sample #4: contains carbon ~61 wt%, iron ~16 wt%, chromium ~3 wt%, sodium ~2 wt%, magnesium ~2 wt%, zinc ~1 wt%, calcium ~1 wt%, and other elements.

Sample #5: contains carbon ~31 wt%, iron ~12 wt%, sodium ~11 wt%, calcium ~6 wt%, magnesium ~6 wt%, zinc ~3 wt%, chromium ~1 wt%, and other elements.

Sample #6: contains iron ~32 wt%, carbon ~27 wt%, aluminium ~5 wt%, sodium ~2 wt%, zinc ~1 wt%, calcium ~1 wt%, magnesium ~1 wt%, and other elements.

Sample #7: contains carbon ~46 wt%, iron ~18 wt%, magnesium ~7 wt%, calcium ~2 wt%, zinc ~2 wt%, chromium ~1 wt%, sodium ~1 wt%, and other elements.

Sample #8: contains carbon ~22 wt%, iron ~43 wt%, calcium ~13 wt%, sodium ~7 wt%, aluminium ~6 wt%, magnesium ~6 wt%, zinc ~2 wt%, and chromium ~1 wt%.

In this research we performed qualitative and quantitative composition of major chemical elements contained in DPM by means of high-resolution LIBS technique. However, further research is necessary to obtain a detailed picture of additional

major and minor chemical elements also present in DPM, for which our current LIBS setup does not have the spectral resolution, particularly sulphur and chlorine.

All these qualitative and quantitative LIBS studies were performed on DPM collected from in-use Diesel engine passenger vehicles and nonspecial driving test cycles; neither test vehicles nor engine test bench systems were used during the LIBS measurements. Therefore for future measurements of particulate matter and soot emissions, it would be important to perform LIBS qualitative and quantitative measurements on dynamic engine test bench system. The focus should be to study static exhaust emissions at different Diesel engine operating points like power, torque, engine speed, fuel injection, brake specific fuel consumption BSFC, etc. and thus perform engine static map measurements. With these engine data and LIBS analytical results from DPM, it would be possible to establish respective correlations.

All acquired knowledge about Diesel particulate matter can help to better control the engine, as well as combustion process, and thus reduce unwanted emissions generated by Diesel engine-powered vehicles in real driving situations to meet future strict emission standards.

4. Conclusions

In this study we present qualitative and quantitative analytical studies of Diesel particulate matter collected from 67 different in-use, Diesel combustion engine-powered, passenger vehicles. DPM samples have been analysed spectrochemically by means of a high-resolution laser-induced breakdown spectroscopy technique. Selections of Diesel passenger vehicles have been performed randomly, from daily life environment and from major brand car producers in Europe. We found that Diesel particulate matter from in-use vehicles does not consist solely or at least mainly of pure carbon particles. Instead it consists of many chemical elements with diverse concentrations. The high-resolution LIBS technique can instantly measure major chemical elements within the Diesel particulate matter matrix. From qualitative LIBS measurements, we found that the major compounds of DPM are carbon (C), iron (Fe), magnesium (Mg), aluminium (Al), chromium (Cr), zinc (Zn), sodium (Na), and calcium (Ca).

We have shown that the composition of DPM matrices is not fixed but rather variable for particular in-use Diesel engine passenger vehicles. We have shown 3 optical emission LIBS spectra from VUV to VIS spectral region and 67 different spectra from major chemical elements contained in different Diesel particulate matter samples.

We qualitatively compared the carbon, calcium, iron, chromium, sodium, zinc, aluminium, magnesium, oxygen, and hydrogen distribution in DPM from 67 different in-use Diesel engine passenger vehicles by LIBS.

Special concern has been given to the quantification of the LIBS signal obtained from the different DPM matrices. With this intent calibration samples, containing selected major matrix elements with different concentrations, have been prepared from certified nano-powder materials in our laboratory. This way, it was possible to construct calibration curves for C, Fe, Mg, Al, Cr, Zn, Na, and Ca.

By applying calibration curves, we quantitatively characterised eight different Diesel particulate matter samples and their major chemical compositions. We found that the carbon concentration in DPM matrices varies extremely from 64 to 22 wt%. The iron concentration is alternating from 55 to 8 wt% for different DPM samples. Magnesium concentrations rise up to 7 wt%, and aluminium content can be more than 6 wt% in different Diesel particulate matter matrices.

Chromium concentration can reach 6 wt% and zinc concentration 7 wt%. In some samples sodium and calcium concentrations are up to 12 wt% or more than 13 wt%, respectively.

In this study we have assessed the qualitative and quantitative compositions of major elements within the various DPM matrices using a high-resolution LIBS technique. However, further research is necessary to obtain a detailed picture of additional major elements also present in DPM, for which our current LIBS setup does not have the spectral resolution, particularly sulphur and chlorine. Understanding the chemical composition of Diesel particulate matter can help to better control the engine, as well as combustion process, and thus reduce unwanted emissions generated by Diesel engine-powered vehicles in real driving situations, to meet future emission standards.

Acknowledgements

Author details

Richard Viskup*, Christoph Wolf and Werner Baumgartner
Institute of Biomedical Mechatronics, Johannes Kepler University Linz, Linz, Austria

*Address all correspondence to: richard.viskup@jku.at

IntechOpen

References

[1] Ntziachristos L, Papadimitriou G, Ligterink N, Hausberger S. Implications of Diesel emissions control failures to emission factors and road transport NOx evolution. Atmospheric Environment. 2016;**141**:542-551. DOI: 10.1016/j.atmosenv.2016.07.036

[2] Zacharof N, Tietge U, Franco V, Mock P. Type approval and real-world CO2 and NOx emissions from EU light commercial vehicles. Energy Policy. 2016;**97**:540-548. DOI: 10.1016/j.enpol.2016.08.002

[3] Commission Regulation (EU) 2016/646. Commission Regulation (EU) 2016/646 of 20 April 2016 Amending Regulation (EC) (No 692/2008) as Regards Emissions from Light Passenger and Commercial Vehicles (Euro 6) [Online]. Available from: http://eur-lex.europa.eu/eli/reg/2016/646/oj

[4] Commission Regulation (EC) 692/2008. Commission Regulation (EC) 692/2008 of 18 July 2008 Implementing and Amending Regulation (EC) No 715/2007 of the European Parliament and of the Council on Type-approval of Motor Vehicles with Respect to Emissions from Light Passenger and Commercial Vehicles (Euro 5 and Euro 6) and on Access to Vehicle Repair and Maintenance Information [Online]. Available from: http://eur-lex.europa.eu/eli/reg/2008/692/oj

[5] Regulation (EC) No 715/2007. Regulation (EC) No 715/2007 of the European Parliament and of the Council of 20 June 2007 on Type Approval of Motor Vehicles with Respect to Emissions from Light Passenger and Commercial Vehicles (Euro 5 and Euro 6) and on Access to Vehicle Repair and Maintenance Information [Online]. Available from: http://eur-lex.europa.eu/eli/reg/2007/715/oj

[6] United States Environmental Protection Agency, Regulations for Emissions from Vehicles and Engines, Tier 3 Motor Vehicle Emission and Fuel Standards [Online]. Available from: https://www.epa.gov

[7] California Environmental Protection Agency. Low-Emission Vehicle Program—LEV III [Online]. Available from: https://www.arb.ca.gov/

[8] Lough GC, Schauer JJ, Park JS, Shafer MM, Deminter JT, Weinstein JP. Emissions of metals associated with motor vehicle roadways. Environmental Science & Technology. 2005;**39**(3):826-836. DOI: 10.1021/es048715f

[9] Schauer JJ, Kleeman MJ, Cass GR, Simoneit BRT. Measurement of emissions from air pollution sources. 2. C-1 through C-30 organic compounds from medium duty diesel trucks. Environmental Science & Technology. 1999;**33**(10):1578-1587. DOI: 10.1021/es980081n

[10] Cheung KL, Ntziachristos L, Tzamkiozis T, Schauer JJ, Samaras Z, Moore KF, et al. Emissions of particulate trace elements, metals and organic species from gasoline, diesel, and biodiesel passenger vehicles and their relation to oxidative potential. Aerosol Science and Technology. 2010;**44**(7):500-513. DOI: 10.1080/02786821003758294

[11] Ntziachristos L, Ning Z, Geller MD, Sheesley RJ, Schauer JJ, Sioutas C. Fine, ultrafine and nanoparticle trace element compositions near a major freeway with a high heavy-duty diesel fraction. Atmospheric Environment. 2007;**41**(27):5684-5696. DOI: 10.1016/j.atmosenv.2007.02.043

[12] Kleeman MJ, Schauer JJ, Cass GR. Size and composition distribution of fine particulate matter emitted from motor vehicles. Environmental Science & Technology. 2000;**34**(7):1132-1142. DOI: 10.1021/es981276y

[13] Noll R. Laser-Induced Breakdown Spectroscopy, Fundamentals and Applications. Berlin Heidelberg: Springer-Verlag; 2012. ISBN 978-3-642-20667-2

[14] Miziolek AW, Palleschi V, Schechter I. Laser-induced breakdown spectroscopy (LIBS). In: Fundamentals and Applications. New York, USA: Cambridge University Press; 2006. ISBN 978-0-521-85274-6

[15] Cremers DA, Radziemski LJ. Handbook of Laser-Induced Breakdown Spectroscopy. New Delhi, India: John Wiley & Sons Inc; 2013. ISBN 978-1-119-97112-2

[16] Hahn DW, Omenetto N. Laser-induced breakdown spectroscopy (LIBS), part II: Review of instrumental and methodological approaches to material analysis and applications to different fields. Applied Spectroscopy. 2012;**66**(4):347-419. DOI: 10.1366/11-06574

[17] Noll R, Fricke-Begemann C, Brunk M, Connemann S, Meinhardt C, Scharun M, et al. Laser-induced breakdown spectroscopy expands into industrial applications. Spectrochimica Acta Part B: Atomic Spectroscopy. 2014;**93**:41-51. DOI: 10.1016/j.sab.2014.02.001

[18] Fortes FJ, Moros J, Lucena P, Cabalin LM, Laserna JJ. Laser-induced breakdown spectroscopy. Analytical Chemistry. 2013;**85**(2):640-669. DOI: 10.1021/ac303220r

[19] Wang ZZ, Deguchi Y, Zhang ZZ, Wang Z, Zeng XY, Yan JJ. Laser-induced breakdown spectroscopy in Asia. Frontiers of Physics. 2016;**11**(6):114213. DOI: 10.1007/s11467-016-0607-0

[20] Viskup R, Praher B, Linsmeyer T, Scherndl H, Pedarnig JD, Heitz J. Influence of pulse-to-pulse delay for 532 nm double-pulse laser-induced

breakdown spectroscopy of technical polymers. Spectrochimica Acta Part B: Atomic Spectroscopy. 2010;**65**:935. DOI: 10.1016/j.sab.2010.09.003

[21] Samek O, Beddows DCS, Kaiser J, Kukhlevsky SV, Liska M, Telle HH, et al. Application of laser-induced breakdown spectroscopy to in situ analysis of liquid samples. Optical Engineering. 2000;**39**(8):2248-2262. DOI: 10.1117/1.1304855

[22] Effenberger AJ, Scott JR. Effect of atmospheric conditions on LIBS spectra. Sensors. 2010;**10**(5):4907-4925. DOI: 10.3390/s100504907

[23] Stehrer T, Praher B, Viskup R, Jasik J, Wolfmeir H, Arenholz E, et al. Laser-induced breakdown spectroscopy of iron oxide powder. Journal of Analytical Atomic Spectrometry. 2009;**24**:973-978. DOI: 10.1039/b817279j

[24] Viskup R, Praher B, Stehrer T, Jasik J, Wolfmeir H, Arenholz E, et al. Plasma plume photography and spectroscopy of Fe-oxide materials. Applied Surface Science. 2008;**255**:5215-5219. DOI: 10.1016/j.apsusc.2008.08.092

[25] Viskup R. Single and double laser pulse interaction with solid state—Application to plasma spectroscopy. In: Dumitras DC, editor. Nd:YAG Laser. Rijeka, Croatia: IntechOpen; 2012. ISBN: 978-953-51-0105-5

[26] Pedarnig JD, Heitz J, Ionita R, Dinescu G, Praher B, Viskup R. Combination of RF-plasma jet and laser-induced plasma for breakdown spectroscopy analysis of complex materials. Applied Surface Science. 2011;**257**(12):5452-5455. DOI: 10.1016/j.apsusc.2010.11.112

[27] Noll R, Sturm V, Aydin Ü, Eilers D, Gehlen C, Höhne M, et al. Laser-induced breakdown spectroscopy—From research to industry, new frontiers for process control. Spectrochimica

Acta Part B. 2008;**63**:1159-1166. DOI: 10.1016/j.sab.2008.08.011

[28] Viskup R, Baumgartner W. Measurement of the main compounds present in the diesel particulate matter exhaust emissions generated from the real diesel combustion engine passenger vehicles. In: Proc. SPIE 10680, Optical Sensing and Detection V, 1068017. [Published: 09 May 2018]. DOI: 10.1117/ 12.2307357